2014

Performance Enhancement in Sliding Vane Rotary Compressors through a Sprayed Oil Injection Technology

Giuseppe Bianchi
University of L'Aquila, Italy, giuseppe.bianchi@graduate.univaq.it

Roberto Cipollone
University of L'Aquila, Italy, roberto.cipollone@univaq.it

Stefano Murgia
Ing. Enea Mattei S.p.A., Vimodrone (Milan), Italy, stefano_murgia@mattei.it

Giulio Contaldi
Ing. Enea Mattei S.p.A., Vimodrone (Milan), Italy, giulio_contaldi@mattei.it

Follow this and additional works at: http://docs.lib.purdue.edu/icec

Performance Enhancement in Sliding Vane Rotary Compressors through a Sprayed Oil Injection Technology

Giuseppe BIANCHI[1†], Roberto CIPOLLONE[1*], Stefano MURGIA[2‡], Giulio CONTALDI[2††]

[1] University of L'Aquila,
Department of Industrial and Information Engineering and Economics,
L'Aquila, Italy
[†]giuseppe.bianchi@graduate.univaq.it,
[*]roberto.cipollone@univaq.it, +39 0862 434319

[2] Ing. Enea Mattei S.p.A.,
Vimodrone, Italy
[‡] stefano_murgia@mattei.it, [††] giulio_contaldi@mattei.it

* Corresponding Author

ABSTRACT

In Sliding Vane Rotary Compressors, as well as in most of positive displacement machines, the oil is injected to accomplish sealing and lubrication purposes. However, the oil injection could produce an additional outcome during the compression phase with a great saving potential from the energetic point of view. Being the air inside the cell at a higher temperature than the oil injected, a cooling effect could be achieved so decreasing the mechanical power required for the compression. At the moment, the oil is introduced inside the compressor vanes simply through a series of calibrated holes that are only able to produce solid jets. In this way any effective heat transfer is prevented, as demonstrated by p-V measurements inside the cells during the compression phase.

In the current study, a theoretical model of a sprayed oil injection technology was developed and further experimentally validated. The oil was injected along the axial length of the compressor through a number of pressure swirl atomizers which produced a very fine spray. The conservation equations, solved with a Lagrangian approach, allowed to track the droplets evolution from the injection until the impingement onto the metallic surfaces of the vanes. The theoretical approach assessed the cooling effect due to the high surface to volume ratio of the droplets and a reduction of the indicated power was predicted. The model validation was carried out through a test campaign on an mid-size sliding vane compressor equipped with a series of pressure swirl injectors. The reconstruction of the indicator diagram as well as the direct measurements of torque and revolution speed revealed a reduction of the mechanical power absorbed close to 7% using an injection pressure of 20 bar. The model is in a satisfactory agreement with the tests and it also confirms the experimental trends available in the literature. A parametric analysis on the injection pressure and temperature and on the cone spray angle was eventually carried out in order to identify an optimal set of operating injection parameters.

1. INTRODUCTION

Compressed air accounts for a mean 10 % of the global industrial electric energy consumptions (Radgen, 2001) and this share may reach the 20 % if commercial and residential needs are included (portable tools, air pumps, pneumatic heating, ventilation, air conditioning, etc…) (US Department of Energy and Energy Efficiency and Renewable Energy, 2003). In order to accomplish the global energetic and environmental commitments, energy saving is nowadays recognized as the main action that needs to be put into action. Within this framework, in Compressed Air Systems (CAS) lots of saving measures have been employing with actions upstream and downstream of the compressed air production: pipeline leakages reduction, CAS design, adjustable speed drives, optimization of the end use devices, frictional losses, etc. As concerns the compressor technology, the saving potential was estimated to be around the 10-20 % (740 TWh in 2012) (Cipollone and Vittorini, 2014). In industrial applications, rotary volumetric machines are the most widespread technology in the range 7-12 bar and flow rates less than 1000 m^3/min with an electrical power

from a few kW to several hundred kW. Among them, Sliding Vane Rotary Compressors (SVRC) represent only few points percent of the overall market. However, they have some intrinsic features which state an unforeseen potential. Indeed, a recent study on the energy reduction perspectives in positive displacement machines stated that SVRCs behave more efficiently than screw compressors if on\off load conditions were taken into account while estimating the energy consumptions (Cipollone, 2014). In order to additionally increase the premium performance of SVRCs, a thermodynamic improvement was highlighted approaching the current adiabatic transformation towards an isothermal one by means of a sprayed oil injection technology that preliminary demonstrated its ability to internally cool the air during the compression phase (Cipollone et al., 2012, 2013).

The performance enhancement through a sprayed oil injection technology has been assessed almost exclusively on screw compressors. Mathematical models on the heat transfer between oil droplets and air have been set up by Seshaiah et al. (2007) and Stosic et al. (1988) as well as experimental activities on the sole atomizers (Paepe et al., 2005) or the whole compressor test rig have been carried out (Stošić et al., 1992; Fujiwara and Osada, 1995), even using different working fluids (Seshaiah et al., 2010). Among them, Stošic et al. (1992) stated a reduction on the energy consumptions from 2.8 % to 7.4 %. The roles of the main injection parameters have been investigated: injection pressure and temperature, oil flow rate, orifice diameter (Paepe et al., 2005), injectors positioning (Ferreira et al., 2006), etc.

In the current work, the Authors pursued the investigation of the effects due to spraying the oil in sliding vane compressors presenting a comprehensive theoretical model for the axial injection. The model was further validated through tests on a mid-size SVRC equipped with pressure swirl nozzles. A series of piezoelectric pressure transducers allowed to assess an overall matching between the simulations and the experimental indicator diagram (p-V). A parametric analysis on the main injection operating parameters eventually addressed further improvements to the innovative injection technology.

2. AXIAL OIL INJECTION MODELING

The oil sprayed injection was modeled following a lumped parameter approach for the thermodynamics inside the compressor cells while the oil particles were tracked in a Lagrangian framework. The injectors are assumed to be located on a side cover of the machine such that the oil droplets sprayed propagate along the axial direction of the compressor. The model aims at understanding the interactions between oil sprays and the compressing air in order to identify the optimal set of injection parameters to address the experimental activity. To ease the computations without losing the physics behind the model, some assumptions were made: among them, a two dimensional approach was used to detect the spray evolution within the rotating cells. Hence, for each injector at a given angular position, the frame of reference chosen for the study was the radial-axial plane. Furthermore, the way of subdividing the spray in droplets packages having different injection angles also led to neglect secondary phenomena like the droplets coalescence. The overall structure of the model is composed of three main modules which deal with the spray formation, its interaction with the air according to the conservation principles and its effects on the compression, respectively.

2.1 Spray formation

Using pressure-swirl atomizers and proper injection pressures, the oil jets breakup in a multitude of droplets having different sizes, as experimentally observed by Valenti et al. (2013). Experiments on the same nozzles by Laryea and No (2004) found that the droplet size distribution resembles the Rosin Rammler function with a Sauter Mean Diameter (SMD) estimated according to the empirical correlation in Equation 1 proposed by Liu (1999).

$$SMD = 4.52 \left(\frac{\sigma_o \mu_o^2}{\rho_a \Delta p} \right)^{0.25} \left[2.7 \left(\frac{D_{or} \dot{m}_o \mu_o}{\rho_o \Delta p} \right) \cos \gamma \right]^{0.25} + 0.39 \left(\frac{\rho_o \mu_o}{\rho_a \Delta p} \right)^{0.25} \left[2.7 \left(\frac{D_{or} \dot{m}_o \mu_o}{\rho_o \Delta p} \right) \cos \gamma \right]^{0.75} \tag{1}$$

being γ the half the cone spray angle, D_{or} the orifice diameter and Δp the pressure difference across the nozzle. The latter parameter not only depends on the injection pressure but also on the injectors positioning: as they move towards the end of the compression phase, the air pressure increases and leads to smaller Δp, thus greater SMD.

The thermo-physical properties of the lubricant were evaluated using semi-empirical correlations (Conde, 1996; Mermond et al., 1999; Lottin et al., 2003) tuned with the experimental data from the oil manufacturer: specific gravity 0.95, kinematic viscosity 99 cSt at $40°C$ and 10.2 cSt at $100°C$.
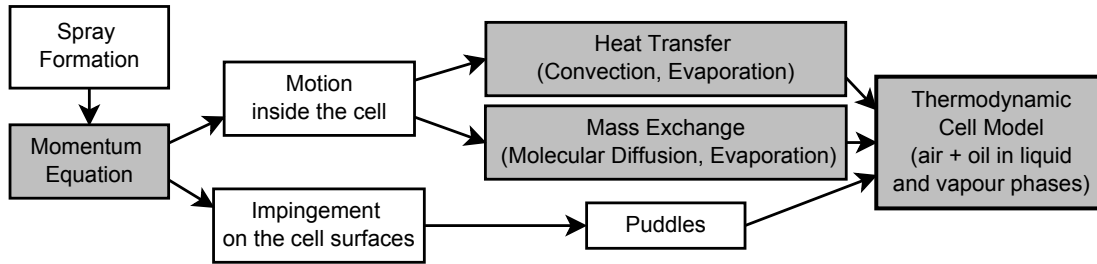
Figure 1: Model scheme

With reference to the same rotating cell, for each atomizer the injection starts when the first blade with respect to the direction of rotation encounters the injector and ends when the second blade leaves it. Therefore, the single injection duration depends on the number of cells and on the angular velocity. If multiple injectors are installed along the angular displacement of the compression phase, the duration is imposed by the overlapping of the first and last injectors, as reported in Equation 2

$$\Delta t_{inj}: \qquad \frac{2\pi}{n\omega} \quad (n_{inj} = 1) \qquad \frac{1}{\omega}\left[\theta_{inj,last} + \frac{2\pi}{n} - \theta_{inj,1st}\right] \quad (n_{inj} > 1) \qquad (2)$$

The oil mass supplied was equally distributed in N_t sub-injections sequentially spaced in time. In each sub-injection, the droplet size distribution was further discretized in N_d parcels that grouped diameter classes close to each other. Each parcel had a different initial direction, chosen according to a Gaussian density distribution. The assumed cone angle was that containing a $\pm 3\sigma$ amplitude on each side of the spray center line to simulate the spray density variation along transverse direction. The initial velocity of all particles, according to Chen et al. (1993) and Laryea and No (2004), was set equal to the jet velocity while the initial temperature of all the droplets equal to the one of the oil downstream the cooler (available from experimental data).

2.2 Interaction between Oil droplets and Air

After the breakup, each of the N_d parcels of oil droplets travels inside the compressor cells whose volume variation influences the thermodynamic properties of the medium in which the spray propagates. In order to study how the oil droplets interacted with the compression process, a coupling of the conservation equations written in a Lagrangian form was adopted according to the scheme in Figure 1. The time in which an effective heat transfer between the oil and the air occurs is equal to the residence time of the oil as droplets i.e. from the spray breakup until the impingement on the metallic surfaces of the cell. Afterwards, the liquid oil film that builds up on the vane surfaces doesn't succeed to affect the compression anymore, as it happens in the current injection technology (liquid jets).
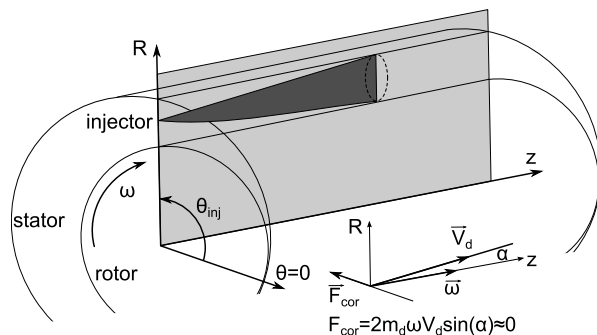

$$\vec{V_d}\frac{dm_d}{dt} + m_d\frac{d(\vec{V_d})}{dt} = \vec{F}_{drag} + \vec{F}_{centrifugal} \qquad (3)$$

$$\vec{F}_{drag} = -\frac{\pi}{8} C_d d_d^2 \rho_a (\vec{V_d})^2$$

$$\vec{F}_{centrifugal} = m_d \omega^2 \vec{R}$$

Figure 2: Reference plane

In order to track the droplets trajectories, the momentum equation was applied in the radial-axial frame of reference relative to each injector $(R, z, \theta_{inj,i})$, as shown in Figure 2. In the most general approach, a droplet that moves in air is subjected to aerodynamic forces (drag and shear lift), inertial and fictitious forces (virtual mass, Bassett history,

centrifugal, Coriolis), volume forces (gravity and buoyancy) and pressure forces (Aggarwal and Peng, 1995). With reference to previous studies, most of these contributions become negligible when compared with the drag, centrifugal and Coriolis forces (Cipollone et al., 2012; C.N. Brown, 1991). Moreover, since the droplets propagate along the R-z plane, the Coriolis force doesn't lie on the frame of reference but its perpendicular to it. However, its magnitude depends on the angle between the droplet velocity and the angular velocity vector that cannot exceed the half of the cone spray angle. Due to the tightness of the gap between stator and rotor, for axial injections nozzles with narrow cone spray angles should be used to prevent that most of the spray would suddenly impinge on the cell surfaces. In accordance with this assumption, the effects of the Coriolis force on the droplets trajectories were neglected and the final expression for the momentum equation became the one reported in Equation 3, whereas the droplet evaporation was taken into account in the term $\vec{V}_d \, dm_d/dt$.

As long as the droplets travel within the compressor cells, they exchange mass and heat with the air. Moreover, depending on the oil saturation pressure at the cell temperature, evaporation or even condensation might occur. From an energetic point of view, the first phase change enhances the air cooling but, at the same time, provides oil vapors that need to be compressed as the air does so leading to an increase of the useful specific work per unit air. On the other hand, if saturation conditions were established inside the cell, the oil vapors would condensate releasing the latent heat to the air with an increase of the compression work as well. Therefore, the target to reach with the sprayed injection technology is to maximize the heat transfer between oil and air without reaching any oil phase change. The overall heat transfer between oil and air was modeled according to the energy equation for the droplet:

$$\frac{d}{dt}\Big[m_d \, c_{p_d}(T_d - T_m)\Big] = \dot{Q}_{a-d} \tag{4}$$

where the subscript *m* refers to the thermodynamic properties of the mixture between air and oil vapors inside the compressor cell whose calculations were performed according to the one-third rule (Abramzon and Sazhin, 2006).

Even if the oil temperature does not reach the boiling conditions, some oil mass may evaporate by molecular diffusion between drop surface and air. According to the Spalding low pressure film evaporation theory, which assumes that the heat and mass exchange between the droplet surface and the gas flow can be modeled as the one occurring within the spherical gas films of constant thickness (Abramzon and Sazhin, 2006), the heat transfer between air and droplet as well as the evaporating mass flow-rate can be calculated solving the energy and mass balance for the region around the droplet (Han et al., 1997). This leads to Equations 5 and 6 respectively:

$$\dot{Q}_{a-d} = \pi \, d_d \, k_m \, N_u^* \, (T_a - T_d) \tag{5}$$

and

$$\dot{m}_{ev} = \pi \, d_d \, D_m \, \rho_m \, S_h^* \, \ln(1 + B_M) \tag{6}$$

On the other hand, at the boiling conditions the calculation of $\dot{m}_{ev}$ involves the latent heat λ and leads to:

$$\dot{m}_{ev} = \frac{\dot{Q}_{a-d}}{\lambda} \tag{7}$$

The corrected Nusselt (Nu^*) and Sherwood (Sh^*) numbers, whose correlations are reported in Equation 8, depend on the Schmidt number (Abramzon and Sazhin, 2006) and the heat (B_T) the mass transfer numbers (B_M) formulated by Spalding (1953).

$$Nu^* = \frac{2 + B_T \left(0.552 \, Re^{1/2} \, Pr^{1/3}\right)}{(1 + B_T)^{0.7} \ln(1 + B_T)} \qquad Sh^* = \frac{2 + B_M \left(0.552 \, Re^{1/2} \, Sc^{1/3}\right)}{(1 + B_M)^{0.7} \ln(1 + B_M)} \tag{8}$$

The continuity equation for the oil eventually takes into account the oil phase changes that might occur and the liquid film formation on the metallic surfaces of the cell. Assuming that if condensation occurred that mass would feed the oil film, for a given injector:

$$\dot{m}_{inj} = \dot{m}_{drop} + \dot{m}_{film} + \dot{m}_{ev} \tag{9}$$

In the present application, being the volatility as well as mass diffusivity of the oil used very low and the dimensions of the droplets atomized not enough small to vaporize, the latter contribution assumes a secondary influence. Hence, the overall heat transfer is driven by the forced convection between oil droplets and air.

2.3 Cell thermodynamics

At the moment, the oil injection in sliding vane compressors, as well as in other volumetric machines, accomplishes lubrication and sealing purposes. This latter feature prevents flow leakages between adjacent cells, and through the side covers of the machine. Assuming a perfect sealing, the cell behaves as a closed system with respect to the air that is trapped at the suction end, compressed and eventually discharged. As concerns the gaseous fluids in the vane, the only mass transfers that may occur are the droplets evaporation (positive) or their condensation (negative). Hence, the working fluid inside the cell is a mixture of air and oil vapors that are assumed to behave as a mixture of ideal gases. Furthermore, the cell thermodynamics was investigated with a lumped parameter approach that led to uniform thermodynamic properties (pressure, temperature, composition etc.). The cell pressure was calculated solving the first derivative of the equation of state. On the other hand, the temperature evolution inside the cell was evaluated according to the first law of the thermodynamics neglecting secondary heat transfer phenomena as the one between the air and the oil film whose topology is continuously modified by the blade sliding within the rotor slots and at the contact point between the tip and the inner surface of the stator. Both the quantities involve the condensation flow rate and latent heat. This phase change occurs if the oil vapor mass exceeds the saturation mass at the cell temperature (Cipollone et al., 2012).

3. EXPERIMENTAL VALIDATION

The mathematical model was validated trough tests on a mid-size industrial sliding vane compressor equipped with a series of pressure-swirl nozzles whose features were recently investigated by Valenti et al. (2013). Their visualizations showed a breakup length, i.e. the distance from the nozzle orifice that the liquid jet requires to achieve an atomized regime of droplets, around 20 mm at 2 bar and 60 $°C$. Using semi-empirical correlations, this datum allowed to estimate the orifice diameter of the nozzle in 1 mm. Additional information that became the input parameters for the model were the half of cone spray angle ($\gamma = 40°$) and the nominal flow rate (2.0 – 2.5 l/min at $\Delta p = 10\,bar$).

The validating test case refers to an experimental activity carried out by Cipollone et al. (2013). The compressor performances were investigated through a series of piezoelectric pressure transducers that allowed to reconstruct the indicator diagram of the machine (p-V). Furthermore, the direct measurements of torque and revolution speed allowed an accurate estimation of the mechanical efficiency of the compressor. Figure 3 reports the test layout with the air, cooling water and oil paths. In the conventional injection technology, the oil is supplied through calibrated holes along the axial length of the compressor thanks to the pressure difference between the oil tank (whose value is close to the discharge pressure) and the cell one at the injectors location (248°). On the contrary, the spray injection technology involved a distributed positioning of the five nozzles on both the side covers of the compressor, as shown in Figure 4. Furthermore, to boost the injection pressure, a gear pump was used to achieve finer atomizations. In both the cases, downstream the compressor outlet the oil is separated from the mixture with air, recycled and cooled to be injected again. The operating conditions for the reference test case are listed in Table 1.

Table 1: Test parameters

	ω	p_{outlet}	oil flow rate	p_{inj}	T_{inj}	air mass flow rate	indicated power	shaft power
	RPM	bar_a	*l/min*	*bar*	$°C$	*kg/s*	*kW*	*kW*
oil spray	1498	8.5	31	20.2	60	0.07	19.4	21.4
oil jets	1500	8.5	37	7.9	67	0.069	20.9	23.1

Figure 5 shows the comparison between the experimental data and the compression trend calculated with the model in the pressure-volume diagram. The duration of each injection is also expressed in terms of volume ranges at the middle right of the chart. The overlapping of the injection ranges led to a superposition of the effects associated to each injector that implied an enhanced heat transfer. The effectiveness of the innovative oil injection technique can be noticed both from experimental and theoretical viewpoints. The blue trace represents the indicator diagram at the same operating point but with the conventional injection technology (oil jets at 8 bar). As can be observed from the
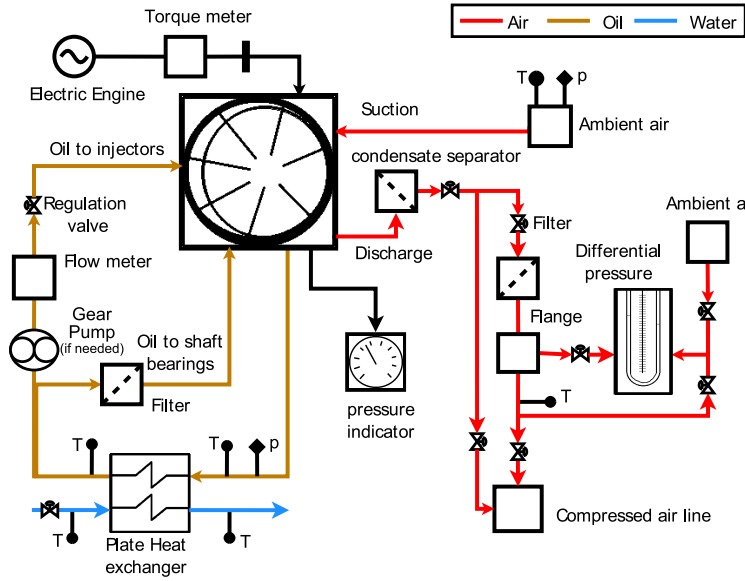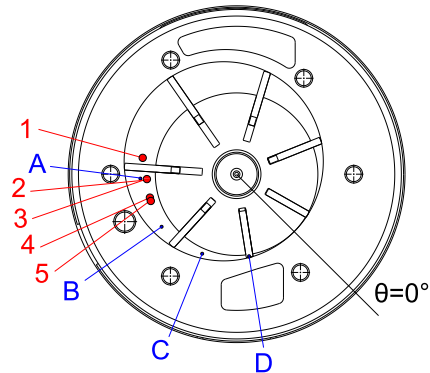
Figure 3: Test Layout

# inj	θ	# piezo	θ
1	215°	A	228°
2	228°	B	260°
3	228°	C	292°
4	240°	D	324°
5	244°		

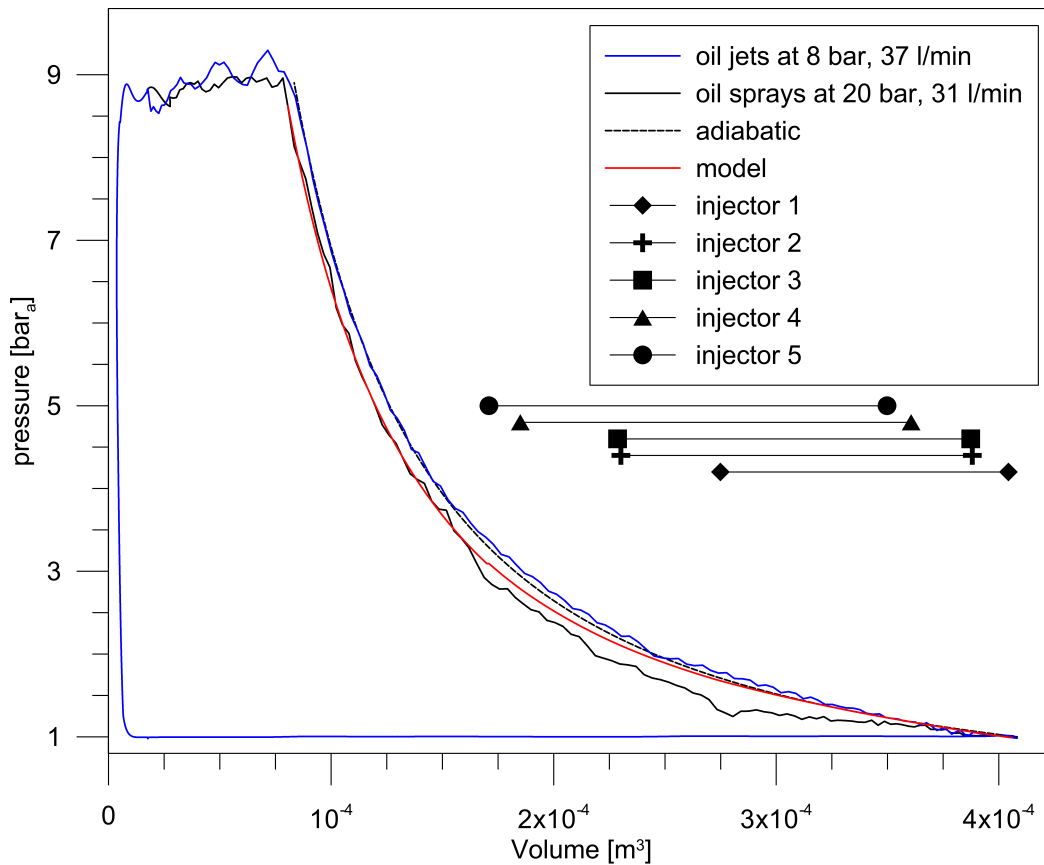**Figure 4: Injectors and piezoelectric sensors positioning**

Figure 5: Comparison between the current injection technology and the sprayed one through experimental indicator diagrams and theoretical compression trends
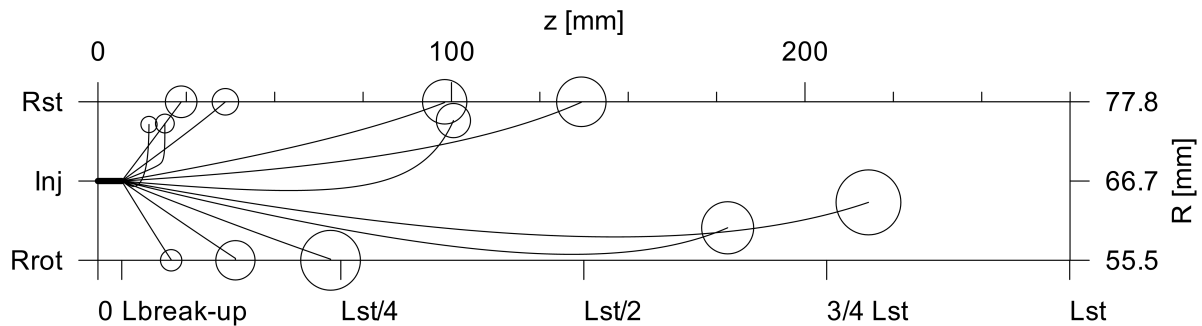
Figure 6: Spray propagation along the axial length of the compressor at $\theta = \theta_{inj,1} = 215°$ **– the chart is in scale while the circles are proportional to the diameter of the droplets**

overlapping with the dashed line, in this case the compression phase is adiabatic. On the other hand, the black line below the adiabatic trend represents the indicator diagram affected by the heat exchange due to the oil sprays. The area between the black and blue curves is the energy saving achieved. The gap between the adiabatic and polytropic trends increases in correspondence of the overlapping of multiple injections while becomes constant after the injection end. Therefore, as the cooling effect ends, the compression becomes again adiabatic until the discharge takes place. The complexity of the physical phenomena involved in the first part of the injection (droplets collisions and coalescence, 3D sprays) and the assumptions on which the model was developed motivate the mismatching between the experimental and calculated trends. Nevertheless, the model matches the cell pressure reached at the injection end and it is able to follow the pressure evolution in the last part of the compression phase. Although the indicated power is affected by the uncertainty due to the reconstruction of the p-V diagram, an accurate indication of the energy saving benefit achieved is provided by the difference in the mechanical power that is equal to 1.7 kW (7.3 %). This quantity is only due to the cooling effects of the oil and it is not discounted by the energy consumption of the gear pump which is present being the injection pressure higher than the line pressure.

With reference to Figure 6, the simulated droplets trajectories can be observed in the radial-axial plane for the injector #1 at 215.4°. The spray takes place downstream the breakup length of 7 mm, in agreement with the experimental trends available in the literature. After that, the different parcels of droplets propagate with a direction within the nozzle cone spray angle. Depending on the magnitude and direction of the deviation, some of the particles suddenly impinge either on the rotor or on the stator wall. On the other hand, the straight propagation of the packages in the middle of the spray is mainly influenced by the centrifugal force that accelerates the droplets towards the stator. Hence, the magnitude of the deviation is proportional to the square of the revolution speed of the compressor. The drag and inertia forces also affect the droplets motion. Big droplets have a higher inertia that delays the decelerating effects of the drag and the deviation due to the centrifugal force such that they tend to travel along the whole axial length of the compressor. Conversely, the small droplets deviate quite soon.

From a heat transfer point of view, the small droplets have a higher surface to volume ratio and seem to be the most suitable ones to enhance the cooling effects of the spray. On the other hand, the residence time for the heat exchange from the breakup until the impingement is short.

4. PARAMETRIC ANALYSIS

Once the simulation platform of the axial oil injection was developed and experimentally validated, a model based analysis was carried out aiming at improving the energy saving features of the oil spray jets addressing the most relevant operating parameters for a further refining of the technique. Among them, the study presented herein focused on the oil pressure and temperature at the injection and on the cone spray angle of the nozzle. Despite the incompressibility of the oil, the first injection parameter is directly related to the energy consumption of the pressurizing device and directly affects the overall efficiency of the system (SVRC + pump). As concerns the oil temperature, its effects are imperative to keep the lubrication features within acceptable operating ranges but also for the injectors positioning: the oil must be always colder than the air at a given angular location. The cone spray angle eventually affects the amount of oil impinged on the cell surfaces without performing an effective cooling. In all the simulations, the injectors positioning
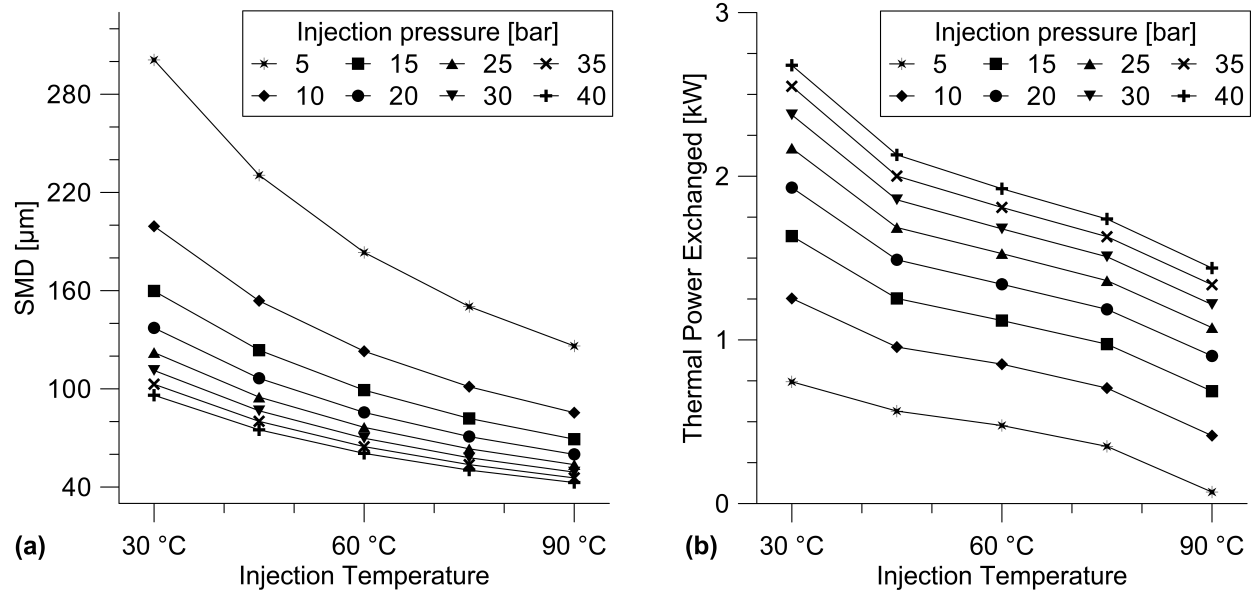
Figure 7: Effects of the oil pressure and temperature at the injection on the spray SMD (a)and on the thermal power exchanged (b)

and the oil rate were kept constant.

Figure 7 analyzes the role that the injection pressure and temperature play on a key indicator concerned to the heat exchange capabilities of the spray, namely the Sauter Mean Diameter (SMD): varying the operating conditions of the injection affects the thermo-physical properties of the oil. In particular, the dynamic viscosity decreases with temperature while the density increases with the injection pressure. Both these facts lead to a finer spray, thus a smaller SMD as reported in Figure 7a. A more prominent influence of the pressure can be noticed: at 60 °C, doubling the pressure from 5 to 10 bar would decrease the SMD from 183 μm to 123 μm and up to 86 μm whether the oil pressure reached 20 bar. Being the trend asymptotical, higher injection pressures do not lead to significant improvements to the SMD reduction thus to overall heat transfer, as Figure 7b shows. In order to achieve a finer spray, the injection temperature could be also increased. However, in this way the temperature difference between oil and compressing air would decrease or even reversed. On the other hand, colder oil injections would enhance the thermal power exchanged up to 30 % going from 60 °C to 30 °C at all the pressure levels simulated. Since in current machines the oil is pressurized by the compressor itself, a maximum value for the oil pressure should be fixed and set equal to the line pressure. In this way, the auxiliary pump could be avoided and the energy benefit (from the enhanced heat transfer) would become net. Feeding the injectors with oil at 10 bar, close to the usual line operating pressure, and at 70 °C, the SMD would stay around 120 μm and the cooling effect in this machine would be close to 1 kW.

Figure 8a reports the non-dimensional rate of growth of the liquid film due to the impingement of the droplets onto the metallic surfaces of the compressor vanes. The analysis was carried out varying the nozzle cone spray angle (2γ) at the same oil rate of the test conditions. In order to keep the same deviation induced by the centrifugal effects, the revolution speed was also kept constant. At all the cone apertures, after the breakup the droplets propagate within the cone spray whose cross section increases along the axial direction (z) until the outer particles reach the stator and rotor surfaces, as presented in Figure 6. Wide cone angles lead to steeper and bigger film formations. Although the puddles build up almost immediately, the film establishment can be delayed narrowing the spray. The steep growth of the film is damped by the oil supplied through injectors #2 and #3. From this point on, the injections balance the impingements and the rate of growth tends to be stabilized to percentages proportional to γ. The effects of the cone spray angle on the overall thermal power exchanged is reported in Figure 8b that also takes into account the influence of the injection pressure. Due to the tightness of the gap between stator and rotor along the axial length of the compressor, cone angles higher than 40° may reduce the cooling capabilities of the sprays up to 60 %. This decrease is mitigated increasing the injection pressure. Hence, despite strong assumptions were made on the two-dimensional nature of the spray and the absence of coalescence (enhanced in narrow sprays), small cone nozzles (γ around 15°) should be adopted to maximize

(a) Influence on the liquid film formation   **(b) Influence on the thermal power exchanged**
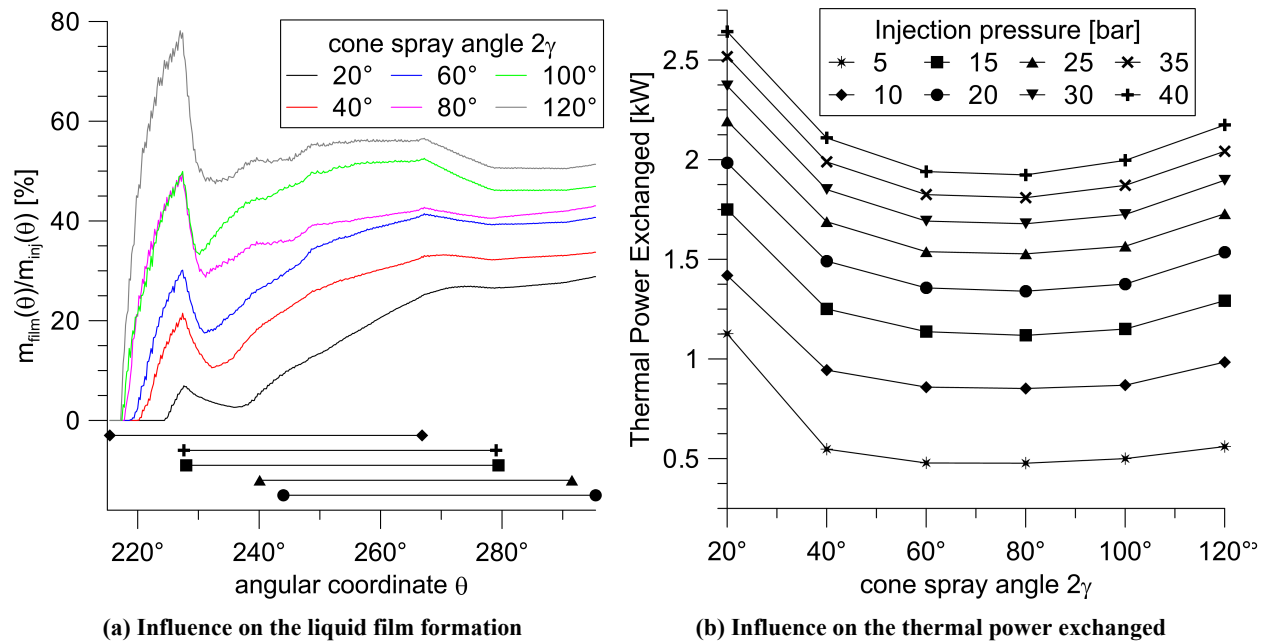
Figure 8: Effects of the cone spray angle on the evolution and cooling capabilities of the sprays

the heat transfer capabilities of the spray in terms of residence time of the oil as droplets.

5. CONCLUSIONS

The current work investigated the energy saving potential of oil spray injections in sliding vane rotary compressors through the enhancement of the heat transfer between oil and air to approach an isothermal compression. A theoretical model of the innovative injection technique was developed. Based on a Lagrangian form of the conservation equations, the model follows the interactions between oil droplets and air from the spray breakup until the impingement on the metallic surfaces of the compressor cells. The effects of multiple injections can be superimposed to increase the cooling effects. The model was further validated through an experimental activity on a mid-size SVRC. The compressor was equipped with a series of pressure swirl nozzles that sprayed the oil pressurized at 20 bar by a gear pump. Thanks to the enhanced heat transfer, a decrease on the mechanical power absorbed of 7.3 % was experimentally noticed. Despite the assumptions made, the overall model agreement with the experimental pressure trace retrieved from piezoelectric pressure transducers mounted on the compressor is satisfactory: the cell pressure at the injection end is matched until the discharge takes place. Furthermore, the spray evolution respects the experimental trends available in literature. In order to find an optimal set for the operating parameters of the injection, a parametric analysis was eventually carried out focusing on the oil pressure and temperature at the injection and the nozzle cone spray angle. Although high pressures lead to finer sprays, an asymptotic trend was noticed: over 20 bar the benefit on the overall thermal power exchanged (air cooling) is not convenient anymore. Moreover, at injection pressures higher than the line value, an auxiliary device is needed to pressurize the oil and the net specific benefit decreases. On the other hand, cold injections could be performed to enhance the cooling more than 30 % increasing the temperature difference between oil and air. To maximize the residence time of the droplets inside the compressor vanes, nozzles with narrow cone angles around 30° should be employed with axial injections. When considering variable speed drive compressors, the influence of the revolution speed on the optimal cone spray angle could be taken into account to evaluate the effects of a different centrifugal force on the droplets deviation towards the stator.

REFERENCES

Abramzon, B. and Sazhin, S. (2006). Convective vaporization of a fuel droplet with thermal radiation absorption. *Fuel*, 85(1):32 -- 46.

Aggarwal, S. K. and Peng, F. (1995). A review of droplet dynamics and vaporization modeling for engineering calculations. *Journal of Engineering for Gas Turbines and Power*, 117(3):453--461.

Chen, J. L., Chen, G., and Wells, M. (1993). Dynamic and static flow analysis of a gasoline fuel injector. *Journal of Engineering for Gas Turbines and Power*, 115(4):750--755.

Cipollone, R. (2014). Sliding vane rotary compressor technology and energy saving. *Proceedings of the Institution of Mechanical Engineers, Part E: Journal of Process Mechanical Engineering*.

Cipollone, R., Bianchi, G., and Contaldi, G. (2012). Sliding vane rotary compressor energy optimization. In *ASME 2012 International Mechanical Engineering Congress and Exposition*, pages 69--80. American Society of Mechanical Engineers.

Cipollone, R., Valenti, G., and Bianchi, G. e. a. (2013). Energy saving in sliding vane rotary compressors. In *Proceedings of 8th International Conference on Compressors and their Systems*, pages 173--182. Institution of Mechanical Engineers.

Cipollone, R. and Vittorini, D. (2014). Energy saving potential in existing compressors. In *Proceedings of the 22nd International Compressor Engineering Conference*. Purdue University.

C.N. Brown, N. L. (1991). A numerical study of fuel evaporation and transportation in the intake manifold of a port-injected spark-ignition engine. *Journal of Automobile Engineering*, 205(3):161--175.

Conde, M. R. (1996). Estimation of thermophysical properties of lubricating oils and their solutions with refrigerants: An appraisal of existing methods. *Applied Thermal Engineering*, 16(1):51 -- 61.

Ferreira, C. I., Zamfirescu, C., and Zaytsev, D. (2006). Twin screw oil-free wet compressor for compression–absorption cycle. *International Journal of Refrigeration*, 29(4):556 -- 565.

Fujiwara, M. and Osada, Y. (1995). Performance analysis of an oil-injected screw compressor and its application. *International Journal of Refrigeration*, 18(4):220 -- 227.

Han, Z., Parrish, S., Farrell, P. V., and Reitz, R. D. (1997). Modeling atomization processes of pressure-swirl hollow-cone fuel sprays. *Atomization and Sprays*, 7(6):663--684.

Laryea, G. and No, S. (2004). Spray angle and breakup length of charge-injected electrostatic pressure-swirl nozzle. *Journal of Electrostatics*, 60(1):37 -- 47.

Liu, H. (1999). 4 - empirical and analytical correlations of droplet properties. In *Science and Engineering of Droplets*, pages 238 -- 314. William Andrew Publishing, Norwich, NY.

Lottin, O., Guillemet, P., and Lebreton, J.-M. (2003). Effects of synthetic oil in a compression refrigeration system using r410a. part i: modelling of the whole system and analysis of its response to an increase in the amount of circulating oil. *International Journal of Refrigeration*, 26(7):772 -- 782.

Mermond, Y., Feidt, M., and Marvillet, C. (1999). Thermodynamic and physical properties of mixtures of refrigerants and oils. *International Journal of Refrigeration*, 22(7):569 -- 579.

Paepe, M. D., Bogaert, W., and Mertens, D. (2005). Cooling of oil injected screw compressors by oil atomisation. *Applied Thermal Engineering*, 25(17–18):2764 -- 2779.

Radgen, P. (2001). *Compressed air systems in the European Union: energy, emissions, savings potential and policy actions*. LOG_X Verlag GmbH.

Seshaiah, N., Ghosh, S. K., Sahoo, R., and Sarangi, S. K. (2007). Mathematical modeling of the working cycle of oil injected rotary twin screw compressor. *Applied Thermal Engineering*, 27(1):145 -- 155.

Seshaiah, N., Sahoo, R., and Sarangi, S. (2010). Theoretical and experimental studies on oil injected twin-screw air compressor when compressing different light and heavy gases. *Applied Thermal Engineering*, 30(4):327 -- 339.

Spalding, D. B. (1953). The combustion of liquid fuels. In *Symposium (international) on combustion*, volume 4, pages 847--864. Elsevier.

Stošić, N., Milutinović, L., Hanjalić, K., and Kovačević, A. (1992). Investigation of the influence of oil injection upon the screw compressor working process. *International Journal of Refrigeration*, 15(4):206 -- 220.

Stosic, N., Kovacevic, A., Hanjalic, K., and Milutinovic, L. (1988). Mathematical modelling of the oil influence upon the working cycle of screw compressors. In *Proceedings of the International Compressor Engineering Conference*. Purdue University.

US Department of Energy and Energy Efficiency and Renewable Energy (2003). *Improving Compressed Air System Performance: a sourcebook for industry*.

Valenti, G., Colombo, L., Murgia, S., Lucchini, A., Sampietro, A., Capoferri, A., and Araneo, L. (2013). Thermal effect of lubricating oil in positive-displacement air compressors. *Applied Thermal Engineering*, 51(1–2):1055 --

1066.

NOMENCLATURE

θ	angular coordinate	(*deg*)	μ	dynamic viscosity	($Pa \cdot s$)	F	force	(*N*)
n	number of cells	(–)	σ	surface tension	(*N/m*)		**Subscripts**	
ω	angular speed	(*rad/s*)	k	thermal conductivity	(*W/m/K*)	a	air	
p	pressure	(*Pa*)	c_p	specific heat at const. p	(*J/kg/K*)	o	oil	
T	temperature	(*K*)	$\dot{Q}$	thermal power	(*W*)	m	air-oil vapor mixture	
m	mass	(*kg*)	d	droplet diameter	(*m*)	ev	evaporation	
$\dot{m}$	mass flow rate	(*kg/s*)	C_d	drag coefficient	(–)	d	droplet	
ρ	density	(*kg/m^3*)	V	droplet velocity	(*m/s*)	inj	injection	